The Journal of Eukaryotic Microbiology

ISOP Published by the International Society of Protistologists

Journal of Eukaryotic Microbiology ISSN 1066-5234

ORIGINAL ARTICLE

Morphology and Morphogenesis of a Novel Saline Soil Hypotrichous Ciliate, *Gonostomum sinicum* nov. spec. (Ciliophora, Hypotrichia, Gonostomatidae), Including a Report on the Small Subunit rDNA Sequence

Xiaoteng Lu[a,b,c,†], Jie Huang[d,†], Chen Shao[a], Saleh A. Al-Farraj[e] & Shan Gao[c]

a The Key Laboratory of Biomedical Information Engineering, Ministry of Education, School of Life Science and Technology, Xi'an Jiaotong University, Xi'an 710049, China

b University of Innsbruck, Research Institute for Limnology, Mondseestr. 9, Mondsee 5310, Austria

c Institute of Evolution & Marine Biodiversity, Ocean University of China, Qingdao 266003, China

d Key Laboratory of Aquatic Biodiversity and Conservation of Chinese Academy of Sciences, Institute of Hydrobiology, Chinese Academy of Sciences, Wuhan 430072, China

e Zoology Department, College of Science, King Saud University, P. O. Box 2455, Riyadh 11451, Saudi Arabia

Keywords
Longfeng Wetland; morphogeny; new species; ontogenesis; terrestrial habitat.

Correspondence
C. Shao, The Key Laboratory of Biomedical Information Engineering, Ministry of Education, School of Life Science and Technology, Xi'an Jiaotong University, Xi'an 710049, China
Telephone/FAX number: +86-29-8266-8463; e-mail: andrews1201@hotmail.com

†Both authors contributed equally.

Received: 30 April 2016; revised 28 January 2017; accepted January 30, 2017.
Early View publication February 28, 2017

doi:10.1111/jeu.12398

ABSTRACT

Morphology, cirral pattern, and morphogenesis of the new saline soil hypotrich, *Gonostomum sinicum* nov. spec. collected from Longfeng Wetland in Daqing, north China, were studied, using detailed live observations and protargol-stained specimens. The new species is characterized as follows: (i) a size in vivo of 100–125 × 30–40 μm, (ii) colorless cortical granules, 0.5 μm across, arranged in short rows, (iii) an adoral zone composed of 28–33 membranelles, (iv) three or four frontoventral rows, one of which extends onto the postoral area, (v) left and right marginal rows composed of 18–27 and 21–35, cirri, respectively, and (vi) usually two transverse cirri. Morphogenesis is as usual for the genus *Gonostomum*, i.e. the cirral primordia II–VI are primary primordia which split into two sets for proter and opisthe in division middle stages, except for anlage I which develops independently. However, the number of frontoventral transverse anlagen is either five or six not only in different individuals but even in proter and opisthe of the same divider. The phylogenetic analyses based on SSU rDNA sequences showed that the genus *Gonostomum* is nonmonophyletic, indicating that the patterns of cirri and dorsal kineties are homoplasious characters. The new species *G. sinicum* nov. spec. is perhaps closely related to *Cotterillia bromelicola* and two congeners.

THE ciliated protozoa are a species-rich and morphologically diverse group (Gao et al. 2016; Huang et al. 2014; Lynn 2008; Zhang et al. 2014). Identification for this kind of organisms is always challenging, especially for hypotrichs, due to their morphological similarities between species, both in terms of living characteristics and cirral patterns (Bourland 2015; Chen et al. 2015a,b; Dong et al. 2016; Fan et al. 2015, 2016; Hemberger 1985; Hu and Kusuoka 2015; Huang et al. 2016; Kumar and Foissner 2015; Li et al. 2016; Lu et al. 2015; Luo et al. 2015; Lv et al. 2015; Pan et al. 2016; Singh and Kamra 2015; Zhao et al. 2015).

The hypotrichous genus *Gonostomum*, established by Sterki (1878) with *G. affine* (basionym *Oxytricha affinis* Stein, 1859) as the type species, is mainly characterized by the position and shape of the oral ciliature as well as by the cirral pattern. At present 13 valid species are affiliated with *Gonostomum* (Berger 2011; Bharti et al. 2015; Foissner 2016; Foissner et al. 2002; Song 1990): *G. strenuum* Engelmann, 1862; *G. algicola* Gellért, 1942; *G. kuehnelti* Foissner, 1987; *G. namibiense* Foissner et al., 2002; *G. albicarpathicum* Vd'ačný and Tirjaková, 2006; *G. paronense* Bharti et al., 2015; *G. bromelicola* Foissner, 2016; *G. fraterculus* Foissner, 2016; *G. halophilum*

Foissner, 2016; *G. lajacola* Foissner, 2016; *G. multinucleatum* Foissner, 2016; *G. salinarum* Foissner, 2016; and *G. caudatulum* Foissner & Heber in Foissner 2016. Owning to its uncertain systematic status, Berger (2011) classified *Urosoma macrostomum* Gellért 1957 as incertae sedis in *Gonostomum*.

In January 2015, an unknown hypotrichous ciliate was isolated from Longfeng Wetland, a district of Daqing in northern China. Observations of its morphology both in vivo and after protargol staining demonstrate that it represents a novel species within the genus *Gonostomum*. In this paper, we describe its morphology and morphogenesis. The small subunit ribosomal DNA (SSU rDNA) of the new isolate was sequenced and analyzed in order to estimate its phylogenetic position.

MATERIALS AND METHODS

Sample collection, observation, and terminology

Gonostomum sinicum nov. spec. was collected from a saline soil sample (soil percolate salinity ca. 20‰; pH ca. 10) with strong foul smell (very likely sulphide) in the Longfeng Wetland (46°35′30″N, 125°13′08″E), Daqing, northern China, on May 6, 2014 (Supporting Information).

Ciliates were made to excyst by employing the non-flooded Petri dish method (Foissner 2014). Raw cultures were established at room temperature (about 24 °C), using Petri dishes filled with filtered soil percolate. Some squashed wheat grains were added to support microbial growth. Although we could not establish a clonal culture, the specimens used for morphological and molecular analyses were very likely conspecific because no other *Gonostomum* morphospecies were found during live observations and in the protargol preparations.

The isolated cells were observed in vivo, using bright field and differential interference contrast microscopy. The protargol staining method of Wilbert (1975) was used to reveal the nuclear apparatus and the ciliary pattern. Counts and measurements of stained specimens were performed at a magnification of 1,000X. Drawings of stained cells were made with the aid of a camera lucida. To illustrate the changes occurring during morphogenesis, the old (parental) ciliary structures are depicted by contour, whereas new structures are shaded black. For general and specific terms, see Berger (2011).

DNA extraction, PCR amplification, and sequencing

Ten cells were isolated from the ciliate cultures and washed three times with filtered water (0.22 μm) to remove potential contamination. These cells were then separated into four groups, one each contains one, one, three and five cells. Each of the groups was subsequently transferred to a 1.5 ml microfuge tube with a minimum volume of water. Genomic DNA was extracted separately from these four groups, using Dneasy Blood & Tissue Kit (Qiagen, Hilden, Germany), following the manufacturer's instructions. The PCR was amplified by PremixTaq (Takara Biotechnology Co., Ltd., Dalian, China, ExTaq version cat. no. DRR003A), with primers 18S-F (5′-AAC CTG GTT GAT CCT GCC AGT-3′) and 18S-R (5′-TGA TCC TTC TGC AGG TTC ACC TAC-3′) (Medlin et al. 1988).

Phylogenetic analyses

In order to reveal a more reliable and robust phylogeny, we performed preliminary maximum likelihood (ML) analyses with different ingroup and outgroup taxa (e.g. 67, 77, 88, 76, 103 species). Based on these preliminary analyses, a set of 68 SSU rDNA sequences was used in the final study, including sequences of *G. sinicum* nov. spec., 49 spirotrichs, and 16 closely related environmental samples as well as two urostylids (*Diaxonella trimarginata* and *Urostyla grandis*) as outgroup (see Fig. 7 for accession numbers). Sequences were aligned, using MUSCLE with the default parameters on the GUIDANCE server (Penn et al. 2010). Ambiguous regions and gaps were then removed by Gblocks 0.91b with all three options checked for a less stringent selection (Castresana 2000; Talavera and Castresana 2007). Further modifications were made manually, using BioEdit 7.0 (Hall 1999) resulting in a matrix of 1,722 characters (Supporting Information). The ML analyses were conducted with RAxML-HPC2 v.8 on XSEDE (8.2.4) (Stamatakis et al. 2008) on the CIPRES Science Gateway. Branch nodal support came from 1,000 bootstrap replicates. The program MrModeltest v.2.0 (Nylander 2004) selected the GTR + I + G as the best model with Akaike Information Criterion (AIC), which was then implemented into Bayesian inference (BI) analysis. The BI analysis was performed with MrBayes on XSEDE 3.2.6 (Ronquist and Huelsenbeck 2003) with a run of 4,000,000 generations at a sampling frequency of 100 and a burn-in of 10,000 trees. All remaining trees were used to calculate posterior probabilities, using a majority rule consensus tree. SeaView v.4 (Gouy et al. 2010) and MEGA 6.0 (Tamura et al. 2013) were used to visualize tree topologies.

RESULTS

Description of *Gonostomum sinicum* nov. spec

Body size 100–125 × 30–40 μm in vivo, usually 110 × 35 μm. Length:width ratio about 3.1:1 in vivo, whereas 2.3:1 in protargol stain. Body flexible, but not contractile. Outline in ventral view elliptical with both ends more or less narrowly rounded (Fig. 1A, 2A–D). Ventral side frequently slightly concave, dorsal one slightly convex, dorsoventrally flattened about 2:1. Two ellipsoidal macronuclear nodules longitudinally orientated along cell's main axis or slightly left of it in the anterior and posterior cell halves, about 22 × 12 μm in size (in protargol preparations), length:width ratio of individual nodules about 2.0–2.5:1. Usually two micronuclei (3 μm across). Contractile vacuole about 8 μm across, posterior to buccal vertex, near cell midline; collecting channels not observed (Fig. 1A, 2C). Cortical granules colorless, about 0.5 μm

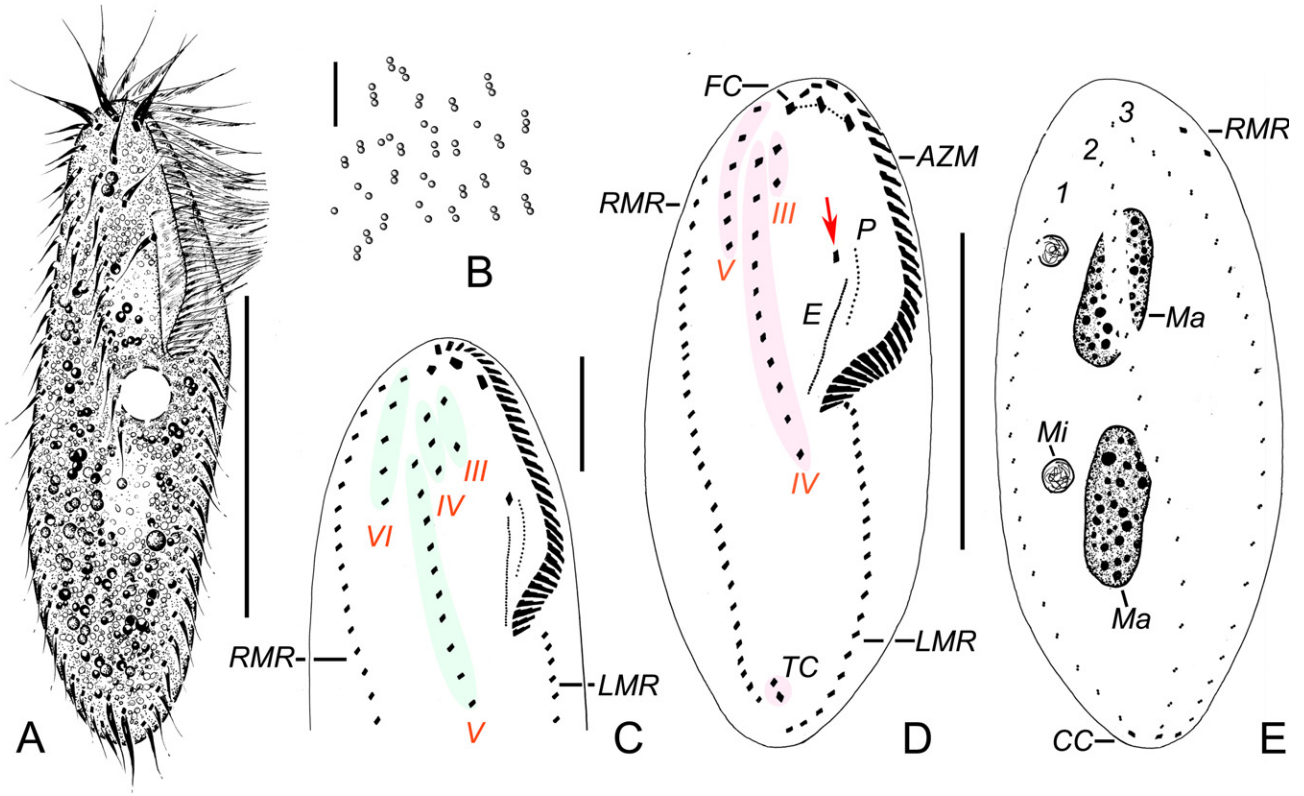

Figure 1 Morphology and infraciliature of *Gonostomum sinicum* nov. spec. in vivo (**A, B**) and after protargol staining (**C–E**). (A) Ventral view of a representative individual. (B) Arrangement of cortical granules. (C) Ventral view showing the frontoventral ciliature. Colored regions mark the four frontoventral rows. (D, E) Ventral (D) and dorsal (E) views of holotype specimen. Colored regions in (D) denote the three frontoventral rows; arrow marks the buccal cirrus. AZM, adoral zone of membranelles; CC, caudal cirri. E, endoral; FC, frontal cirri; LMR, left marginal row; Ma, macronuclear nodules; Mi, micronuclei; P, paroral; RMR, right marginal row; TC, transverse cirri; III–VI (frontoventral rows 1–4), frontoventral rows originating from anlagen III–VI; 1–3, dorsal kineties 1–3; Scale bars = 60 μm (A, D, E); 5 μm (B); 25 μm (C).

across, arranged in short longitudinal rows with usually two or three granules (Fig. 1B, 2E). In protargol-stained specimens, 2–3 μm long spindle-shaped extrusomes in lateral portion of cell cortex (Fig. 2F); we cannot exclude that these structures are cortical granules altered by the protargol method used. Cytoplasm colorless to grayish, contains numerous lipid droplets (ca. 1–5 μm across) that render cell opaque and dark at low magnification. Swims by rotation about main cell axis or crawls slowly on substrate. Food vacuoles not observed, but cells may feed on bacteria as they usually aggregate around the rice grains.

Cirral pattern of usual variability. Three enlarged frontal cirri with cilia ca. 15 μm long. One buccal cirrus, ca. 10 μm long, close to right anterior portion of the paroral. Three or four frontoventral rows: out of the 25 specimens studied, 12 possessed three rows, whereas 13 possessed four. Frontoventral row 1 commences posteriorly to the right frontal cirrus (III/3) and extends in anterior ca. 16% of body length, composed of two cirri (rarely three). In individuals with three frontoventral rows (Fig. 1D, 2G), frontoventral row 2 is the longest, commences right of and slightly behind the anterior cirrus of frontoventral row 1 and extends in anterior cell half reaching the postoral area, composed of an average of ten cirri; frontoventral row 3 (frontoterminal row) starts at the level of the right frontal cirrus and extends in the anterior cell quarter, composed of 5–7 cirri. In individuals with four frontoventral rows (Fig. 1C, 2H), frontoventral row 2 commences slightly posteriorly to the first cirrus of frontoventral row 1 and extends in the anterior cell quarter, composed of about three cirri; frontoventral row 3 is the longest, commences slightly posteriorly to second cirrus of frontoventral row 2 and extends in anterior cell half, extending onto postoral area, composed of an average of ten cirri; frontoventral row 4 (frontoterminal row) starts at about level of right frontal cirrus and extends in the anterior cell quarter, composed of five or six cirri. One right and one left marginal row. Right marginal row commences at level of first cirrus of the frontoterminal row and terminates at level of the posterior transverse cirrus, composed of 21–35 cirri. Left marginal row begins at the level of cytostome and terminates near posterior cell end, composed of 18–27 cirri. Usually two transverse cirri near the posterior end of the right marginal row; out of the 25 specimens, three individuals possessed three transverse cirri (Fig. 2G, I; Table 1).

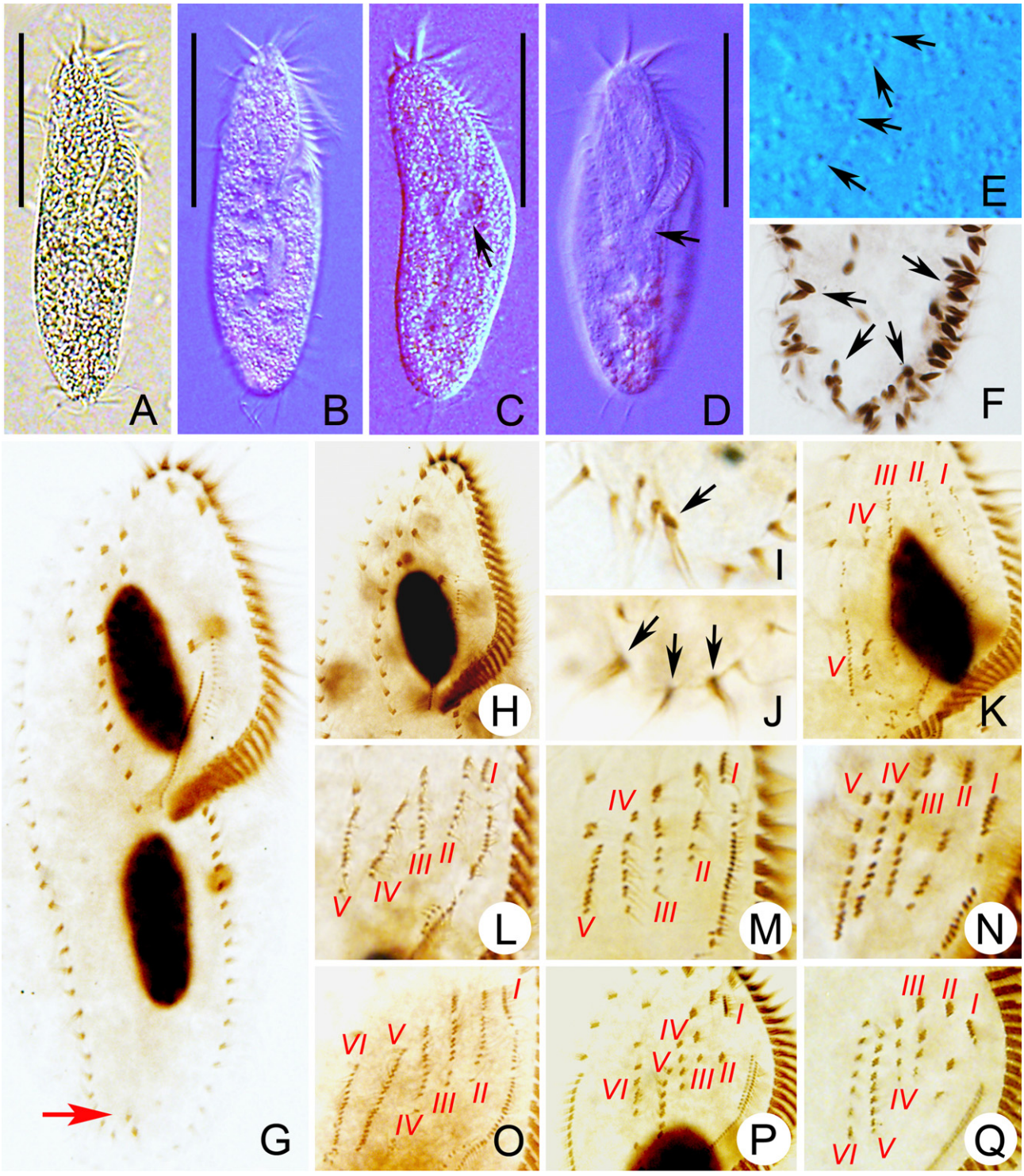

Figure 2 Photomicrographs of *Gonostomum sinicum* nov. spec. from life (**A–E**) and after protargol staining (**F–Q**). (A–D) Different body shapes; arrow in (C) marks the contractile vacuole, in (D) shows the proximal end of the adoral zone. (E) Arrangement of the cortical granules (arrows). (F) The spindle-shaped extrusomes (arrows) after protargol staining. (G) Ventral view of the holotype specimen, arrow marks the transverse cirri. (H) Ventral view showing the frontoventral ciliature. (I) Ventral view showing the three transverse cirri (arrow). (J) Dorsal view showing the three caudal cirri (arrows). (K–M, O, P) Development of frontoventral transverse anlagen in the proter. (N, Q) Development of the frontoventral transverse anlagen in the opisthe. I–VI, frontoventral transverse anlagen I–VI. Scale bars = 60 μm (A–D).

Table 1. Morphometric characterization of *Gonostomum sinicum* nov. spec.

Character[a]	Min	Max	Mean	M	SD	CV	*n*
Body length	96	145	114.8	112	13.37	11.6	25
Body width	38	70	50.1	50	7.73	15.4	25
Body, length: width ratio	1.89	2.89	2.32	2.33	0.27	11.6	25
AZM length	45	68	55.2	55	6.90	12.5	25
AZM length: body length ratio	0.40	0.52	0.48	0.48	0.08	5.9	25
Paroral, length	8	15	11.4	12	1.35	11.9	25
Endoral, length	17	25	20.2	20	1.75	8.9	25
Paroral kinetids, number	10	18	12.2	12	1.80	14.4	25
Anterior body end to begin of paroral, distance	20	30	25.4	25	2.63	10.4	25
Anterior body end to begin of endoral, distance	25	38	30.1	30	3.05	10.1	25
Anterior body end to begin of buccal cirrus, distance	20	32	25.8	25	2.88	10.4	25
Anterior body end to posterior end of frontoventral row 1, distance	12	26	18.8	19	3.59	19.1	25
Anterior body end to posterior end of frontoventral row 2[b], distance	21	33	26.5	27	3.80	14.3	13
Anterior body end to posterior end of frontoventral row 2[c], distance	55	80	67.4	70	7.04	10.4	12
Anterior body end to posterior end of frontoventral row 3[b], distance	50	75	62.0	60	7.63	12.3	13
Anterior body end to posterior end of frontoventral row 3[c], distance	20	40	29.2	30	5.87	20.14	12
Anterior body end to posterior end of frontoventral row 4[b], distance	20	33	28.5	30	4.14	14.5	13
Anterior body end to posterior end of frontoventral row 1, distance: body length ratio	0.12	0.20	0.16	0.16	0.03	15.6	25
Anterior body end to posterior end of frontoventral row 2, distance: body length ratio[b]	0.19	0.30	0.24	0.24	0.03	14.1	13
Anterior body end to posterior end of frontoventral row 2, distance: body length ratio[c]	0.48	0.64	0.56	0.57	0.04	6.85	12
Anterior body end to posterior end of frontoventral row 3, distance: body length ratio[b]	0.50	0.69	0.56	0.55	0.06	10.1	13
Anterior body end to posterior end of frontoventral row 3, distance: body length ratio[c]	0.16	0.30	0.24	0.24	0.04	16.1	12
Anterior body end to posterior end of frontoventral row 4, distance: body length ratio[b]	0.20	0.32	0.26	0.26	0.04	15.0	13
AZM number	28	33	30.2	30	1.26	4.2	25
Buccal cirri, number	1	1	1.0	1	0.00	0.0	25
Frontal cirri, number	3	3	3.0	3	0.00	0.0	25
Transverse cirri, number	2	3	2.1	2	0.33	15.6	25
Frontoventral rows, number	3	4	3.5	4	0.51	14.5	25
Frontoventral row 1 cirri number	2	3	2.0	2	0.20	9.8	25
Frontoventral row 2 cirri number[b]	2	5	3.23	3	0.83	25.75	13
Frontoventral row 2 cirri number[c]	8	11	10.2	11	1.03	10.1	12
Frontoventral row 3 cirri number[b]	5	11	9.6	10	1.61	16.7	13
Frontoventral row 3 cirri number[c]	5	7	5.6	6	0.67	12.0	12
Frontoventral row 4 cirri number[b]	5	6	5.9	6.0	0.38	6.4	13
Total number of frontoventral cirri[d]	10	18	13.9	14	2.02	14.5	25
Right marginal cirri, number	21	35	29.2	30	3.70	12.5	25
Left marginal cirri, number	18	27	21.8	22	2.42	11.1	25
Dorsal kineties, number	3	3	3.0	3	0.00	0.0	25
Dorsal kinety 2, number of kinetids	18	23	20.6	21	1.15	5.6	25
Caudal cirri, number	3	3	3.0	3	0.00	0.0	25
Macronuclear nodules, number	2	2	2.0	2	0.00	0.0	25
Micronuclei, number, number	3	6	3.8	3	1.23	32.6	25
Anterior macronuclear nodule, length	16	28	22.0	22	3.3	15.2	25
Anterior macronuclear nodule, width	9	18	11.6	11	2.22	19.2	25
Micronuclei, length	3	6	3.8	3	1.23	32.6	25
Micronuclei, width	2	5	2.8	3	0.73	26.0	25

[a]All data are based on protargol-stained specimens.
[b]Cells with four frontoventral rows.
[c]Cells with three frontoventral rows.
[d]Frontal cirri, buccal cirrus, and frontoterminal cirri are not included. Measurements in μm.
AZM = adoral zone of membranelles; CV = coefficient of variation in %; M = median; Max = maximum; Mean = arithmetic mean; Min = minimum; *n* = number of cells measured; SD = standard deviation.

Dorsal kineties in *Gonostomum* pattern, i.e. three bipolar dorsal kineties, each with a caudal cirrus at its posterior end; dorsal bristles 3–4 μm long (Fig. 1E, 2J).

Oral apparatus in *Gonostomum* pattern. Adoral zone 45–68 μm long, occupying 40–52% of body length in protargol preparations, composed of 28–33 membranelles with cilia up to 15 μm long. Paroral 8–15 μm long, composed of 10–18 widely spaced monokinetids. Endoral about 20 μm long with densely spaced monokinetids.

Ontogenesis of *Gonostomum sinicum* nov. spec

As usual for the genus *Gonostomum*, the frontoventral transverse cirral anlagen II–VI are primary anlagen, which split into two sets in middle division stages (Berger 2011); so, a distinction between proter's and opisthe's anlagen is not possible in early dividers (Fig. 2K, 3D), except for anlage I, which develops independently and differently.

Stomatogenesis

In the opisthe, the formation of the oral primordium begins with the apokinetal proliferation of basal bodies posterior to the buccal vertex, where a cuneate anarchic field develops (Fig. 3A, B). The formation of membranelles commences at the left anterior end of the oral primordium (Fig. 3D). As the formation of the adoral membranelles proceeds in posterior direction, the anlage

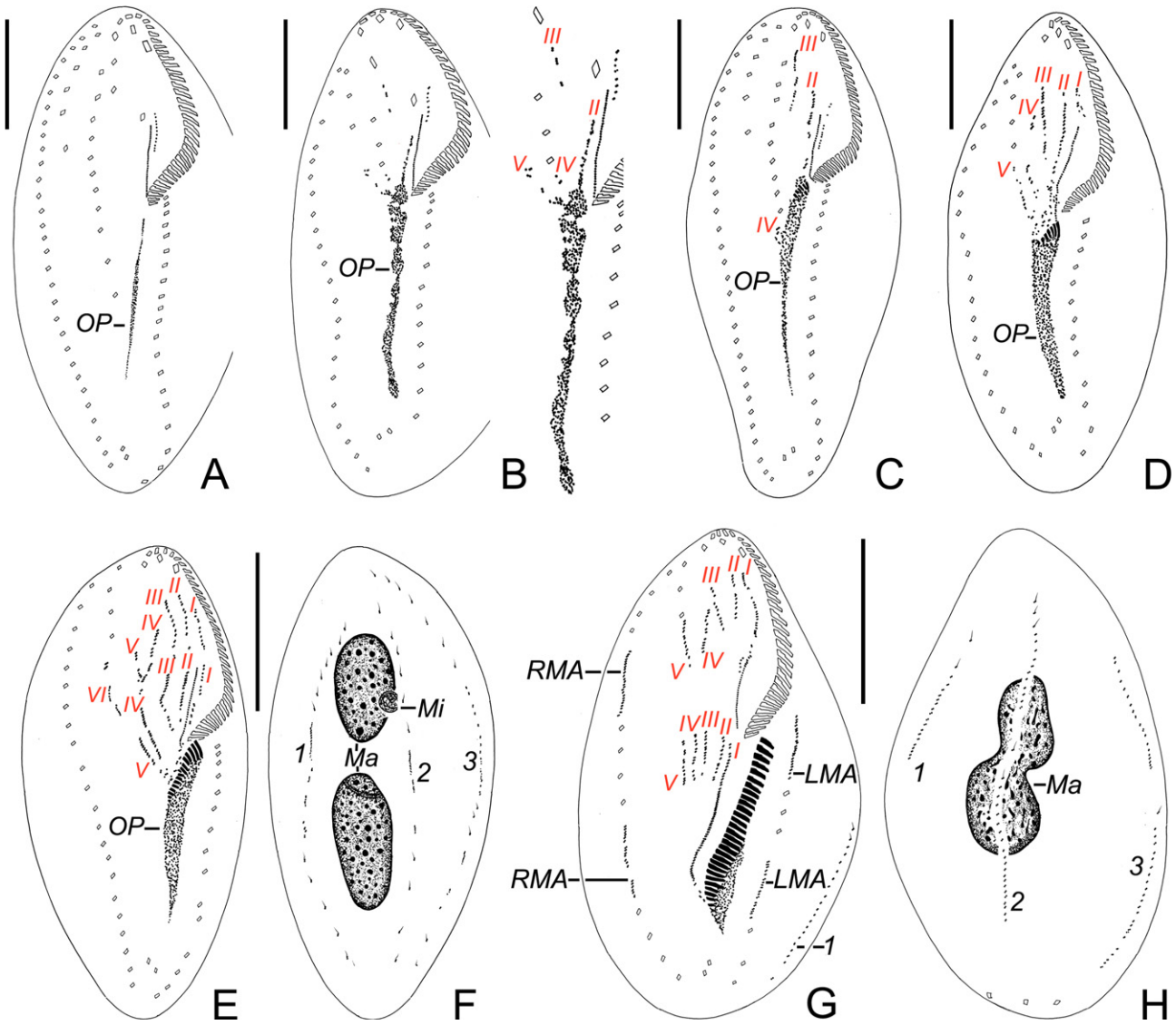

Figure 3 Early and middle stages of morphogenesis and reorganization in *Gonostomum sinicum* nov. spec. after protargol staining. (**A, B**) Ventral views of early dividers. (**C**) An early stage of reorganization. (**D**) Ventral view of an early-middle divider. (**E, F**) Ventral and dorsal views of a middle divider. (**G, H**) Ventral and dorsal views of a later divider. LMA, left marginal anlage; Ma, macronuclear nodules; Mi, micronuclei; OP, oral primordium; RMA, right marginal anlage; I–VI, frontoventral transverse anlagen I–VI; 1–3, dorsal kineties anlagen. Scale bars = 25 μm (A–D); 40 μm (E–H).

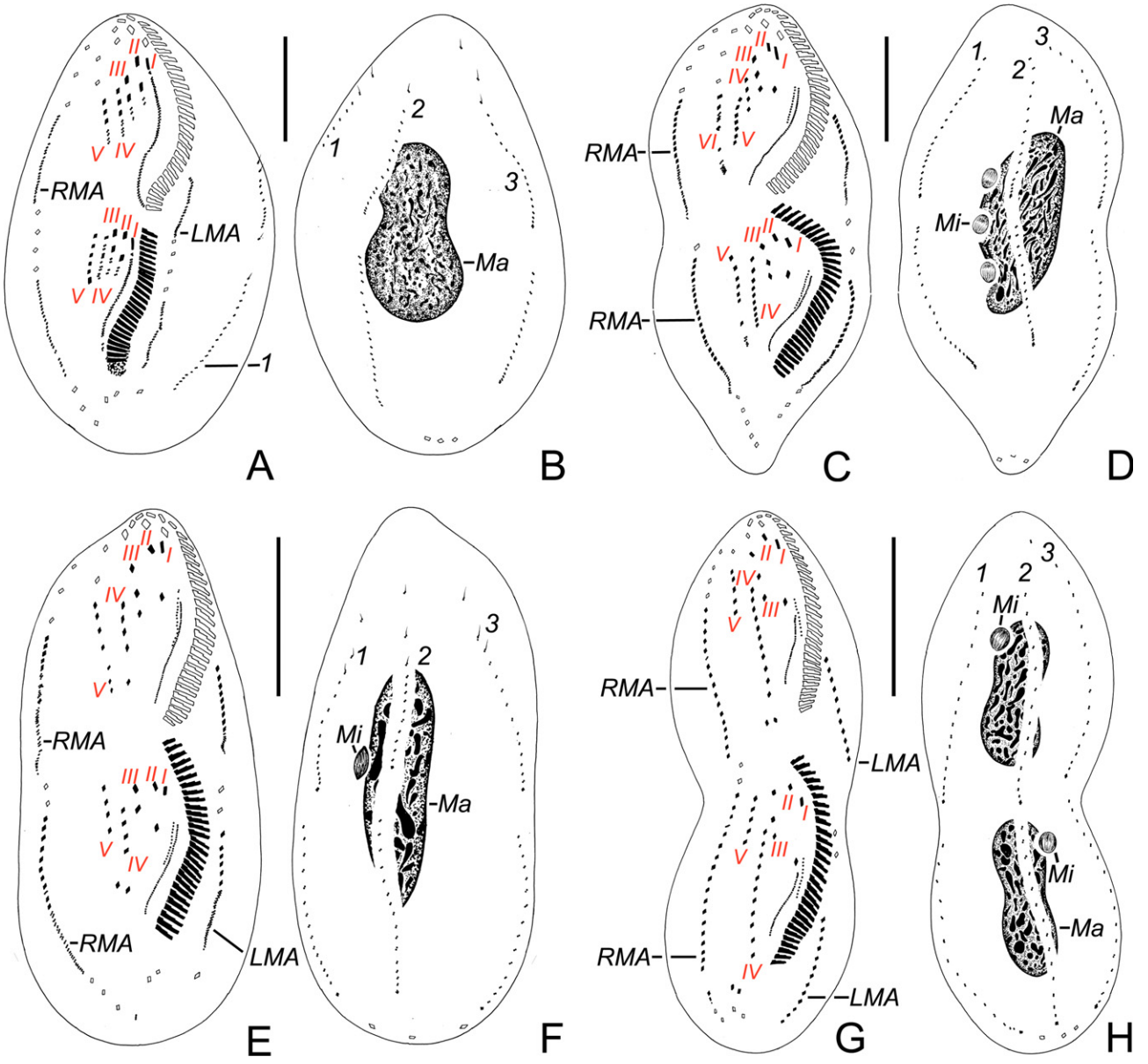

Figure 4 Middle and late stages of morphogenesis in *Gonostomum sinicum* nov. spec. after protargol staining. (**A, B**) Ventral and dorsal views of a middle-late divider. (**C, D**) Ventral and dorsal views of a slightly later divider. (**E, F**) Ventral and dorsal views of a slightly later divider. (**G, H**) Ventral and dorsal views of a late divider. LMA, left marginal anlage; Ma, macronuclear nodules; Mi, micronuclei; RMA, right marginal anlage; I–VI, frontoventral transverse anlagen I–VI; 1–3, dorsal kineties anlagen. Scale bars = 25 μm (A–D); 40 μm (E–H).

for the opisthe's undulating membranes generates as a streak of loosely arranged basal bodies near the right anterior of the oral primordium (anlage I; Fig. 3E). Based on the available dividers, it remains uncertain whether it originates de novo or from the oral primordium. These basal bodies of the undulating membrane anlage arrange to a straight line of dikinetids distinctly separated from the adoral zone, and then the undulating membrane anlage curves leftwards so that a rather wide buccal field is formed (Fig. 2N, 3G, 4A). The anterior portion of the dikinetal line then splits longitudinally, producing a short row of widely spaced basal bodies (the future paroral) to the right and a long row of closely spaced basal bodies (the new endoral) to the left (Fig. 4C, E). When the shaping of the oral apparatus commences, the paroral and endoral incline and move close to the rear half of the adoral zone (Fig. 4C, E). Owing to the shaping of the buccal cavity, the paroral is shifted to the left of the endoral, and morphogenesis of paroral and endoral is complete (Fig. 4G).

In the proter, the parental adoral zone of membranelles is retained (Fig. 3D, E, G, 4A, C, G); changes of the oral structures are confined to the paroral and endoral. The anlage for the undulating membranes (anlage I) is probably formed by the dedifferentiation of the parental paroral, while the parental endoral is gradually resorbed (Fig. 2K, L, 3D, E). In subsequent stages, the basic development of the undulating membranes anlage follows the pattern in the opisthe (Fig. 2M, O, P, 3G, 4A, C, G).

Frontoventral ciliature

While the anarchic field of the oral primordium elongates, the buccal cirrus disorganizes and proliferates basal bodies anteriorly and posteriorly, forming anlage II (Fig. 2K, 3B, D). Simultaneously, the parental frontoventral rows 1–3 disaggregate into basal bodies that proliferate, forming anlagen III and IV together with migrating basal bodies from the anterior end of the oral primordium (Fig. 3B, D). Subsequently, five long streaks (anlagen I-V) are recognizable in the frontal area (Fig. 2K, 3D). The long anlagen (primary primordia) then divide transversely to form two sets of anlagen each for the proter and opisthe (Fig. 3E, G). However, an additional anlage is occasionally formed (i.e. six anlagen in total, Fig. 3E), and thus the number of anlagen ranges from five to six (Fig. 3G, 5A, C). In some dividers, proter and opisthe possess the same number of anlagen (both five or both six) (Fig. 2L–Q, 3G, 4A, E, G), while in other dividers, the proter possesses six anlagen, whereas the opisthe only five (Fig. 3E, 4C). Gradually, cirri segregate from anterior to posterior in the following manner: anlage I produces the frontal cirrus I/1 (left frontal cirrus); anlage II produces the buccal cirrus (II/2) and the frontal cirrus II/3 (middle frontal cirrus); anlage III produces the right frontal cirrus and the frontoventral row 1; anlagen IV and V (IV–VI) produce the frontoventral rows 2 and 3 (rows 2–4), and anlagen n and n−1 produce each one transverse cirrus. Finally, the new cirri arrange in the mature pattern and replace the parental structures. The ciliary patterns of morphostatic individuals (Fig. 1C, D) suggest that the rightmost two rows are homologous, i.e. rows V and VI in Fig. 1C are homologous with rows IV and V in Fig. 1D. Likely, there is an extra anlage formed between III and IV, which gives rise to the additional frontoventral row.

Marginal rows and dorsal kineties

As in congeners, the marginal rows and dorsal kineties form an anlage each in the proter and opisthe by intrakinetal proliferation of basal bodies. Each dorsal kinety will produce one caudal cirrus in the late stage of cell division (Fig. 3E–H, 4A–H).

Division of nuclear apparatus

In an early divider, the replication bands traversed the individual nodules (Fig. 3F). Afterwards, the nuclear apparatus divides in the usual way, i.e. two macronuclear nodules fuse to a single mass during the middle stages and then divide twice prior to cytokinesis. Micronuclei divide mitotically during mid-late stages (Fig. 3H, 4B, D, F, H).

Physiological reorganization

Only one early stage of physiological reorganization was observed, which indicates that the early process of cortical development in reorganizers is similar to cell division.

Phylogenetic analyses based on SSU rDNA sequences

The SSU rDNA sequence of *G. sinicum* nov. spec. has been deposited in GenBank database under the accession number KY475614. The length and GC content of the SSU rDNA sequence are 1,729 nt and 45.63%, respectively. Phylogenetic trees inferred from the SSU rDNA sequences, using two different methods (ML and BI), show similar topologies; therefore, only the ML tree (Fig. 7) is presented with bootstraps and posterior probabilities from both algorithms.

The present phylogeny is far from being robust as indicated by the generally low support values. *Gonostomum sinicum* nov. spec. is the adelphotaxon of *Cotterillia bromelicola* with variable support (ML/BI, 60/0.99). This cluster groups with *G. strenuum*, *G. bromelicola*, one unidentified species of *Gonostomum*, and one unknown species from environmental samples. *Gonostomum namibiense* and *G. paronense* are distinctly separated from their congeners.

DISCUSSION

Comparison with closely related species

In terms of its elongate elliptical, tailless body and two macronuclear nodules, *G. sinicum* nov. spec. should be compared with *G. affine*, *G. strenuum*, *G. algicola*, *Gonostomum* sp. 1 in Shin (1994), *G. halophilum*, *G. salinarum*, *G. lajacola*, *G. bromelicola*, and *G. fraterculus*, *Urosoma macrostomum*, *Metagonostomum gonostomoidum*, and *M. terrestre*.

Gonostomum affine, the type species of *Gonostomum*, contains eight species forming a *G. affine*-complex. However, *G. sinicum* nov. spec. can be separated from *G. affine* by the following features: (i) the number of frontoterminal cirri (5–7 vs. usually two); (ii) the frontoventral row originating from anlage n−1 extends onto the postoral area vs. is confined to the frontal area; (iii) the total number of frontoventral cirri (10–18 vs. 3–7; data from 18 soil populations compiled by Foissner (2000) and Foissner et al. (2001)); (iv) the cortical granules (distinct vs. usually absent or very indistinct); and (v) the left marginal row terminates at the midline of the cell in *G. sinicum* nov. spec. vs. at the level of the transverse cirri in *G. affine* (Fig. 5A; Berger 2011; Berger and Foissner 1988).

Gonostomum sinicum nov. spec. can be distinguished from *G. strenuum* by (i) pretransverse ventral cirri (absent vs. present), (ii) molecular data (27 nucleotides differences between these two species), and (iii) the number of frontoventral rows (three or four vs. invariably four) (Fig. 5B; Berger 2011; Song 1990).

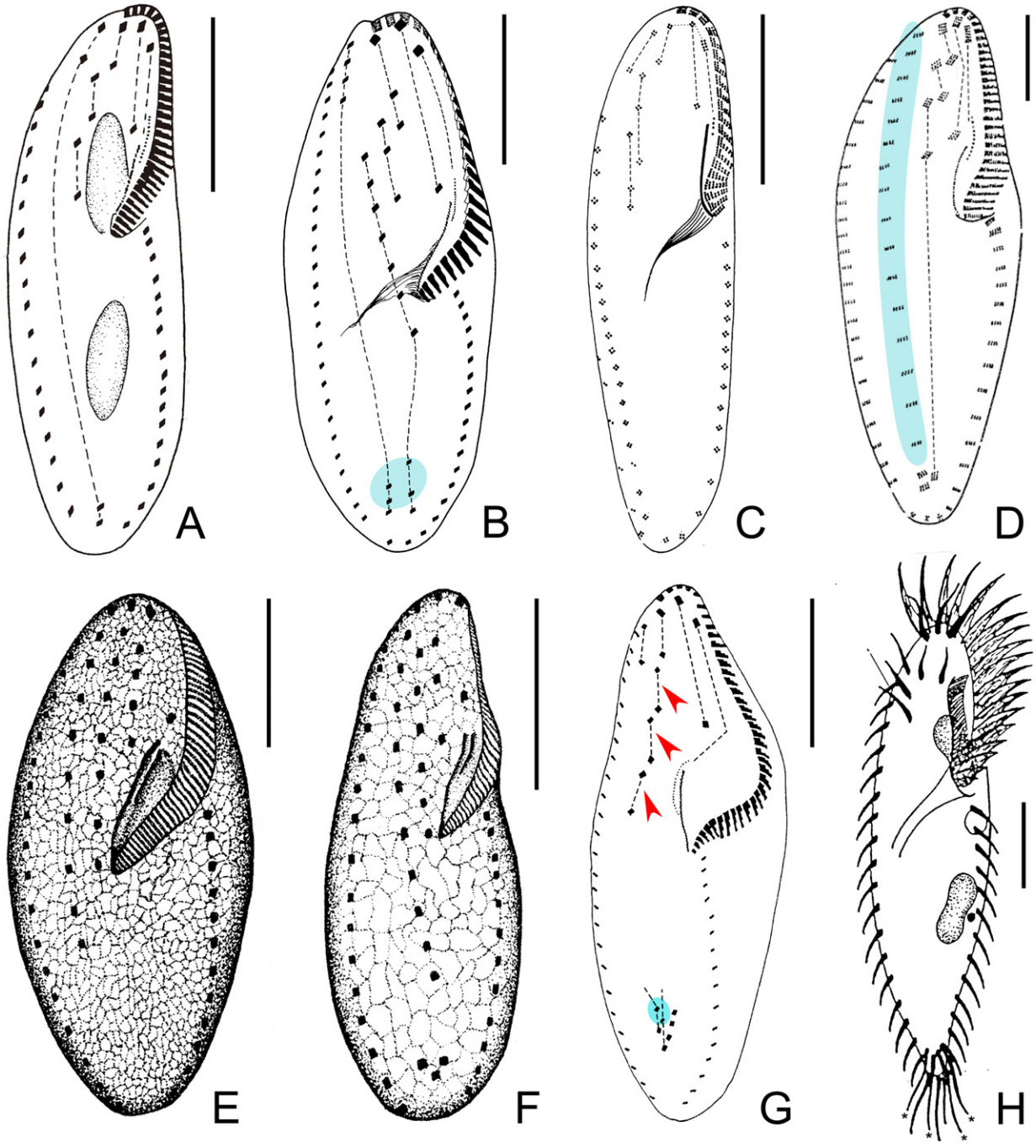

Figure 5 Infraciliature of species related with *Gonostomum sinicum* nov. spec. (**A**) *Gonostomum affine* (from Berger and Foissner 1988). (**B**) *Gonostomum strenuum* (from Song 1990), the region highlighted depicts the pretransverse ventral cirri. (**C**) *Gonostomum algicola* (from Foissner et al. 2002); (**D**) *Metagonostomum gonostomoidum* (from Hemberger 1985), the region highlighted depicts the long rightmost frontoventral row (frontoterminal row). (**E, F**) *Metagonostomum terrestre* (from Alekperov 2005). (**G**) *Gonostomum.* sp. 1 (from Shin 1994), arrowheads indicate the three oblique pseudo-pairs of frontoventral cirri, the region highlighted depicts the pretransverse ventral cirri. (**H**) *Urosoma macrostomum* (from Gellért 1957). Broken lines connect cirri which (very likely) originated from same anlage (Berger 2011). Scale bars = 20 μm (A, C, D); 25 μm (B); 10 μm (E, F, H); 30 μm (G).

Gonostomum sinicum nov. spec. can be separated from *G. algicola* by (i) the body size (100–125 × 30–40 μm vs. 60–110 × 15–30 μm in vivo); (ii) the length of the frontoventral row n−1 (extends onto the postoral area vs. is confined to the frontal area); (iii) the number of frontoterminal cirri (5–7 vs. two or three); (iv) the total number

of frontoventral cirri (ca. 23 vs. 11); (v) the numbers of right (21–35 vs. 15–24) and left (18–27 vs. 10–16) marginal cirri; (vi) the number of adoral membranelles (30 vs. 20 on average); and (vii) the number of paroral basal bodies (10–18 vs. 3–6) (Fig. 5C; Berger 2011; Foissner et al. 2002).

Metagonostomum gonostomoidum differs from *G. sinicum* nov. spec. in its long rightmost frontoventral row (frontoterminal row) with more than ten (vs. 5–7) cirri, extending to the transverse cirri (vs. being confined to the frontal area) (Fig. 5D; Berger 2011; Foissner 2016; Hemberger 1985).

Metagonostomum terrestre is a little-known species because its description is only based on wet silver nitrate impregnation and contains some uncertainties. For instance, *M. terrestre* is reported to have a body length of 30–45 μm, whereas the adoral zone contains 45–50 membranelles; so the number of membranelles does not correspond to the length of the membranellar zone (Fig. 5E, F; Berger 2011). Therefore, the body length of *M. terrestre* provided by Alekperov (2005) is probably incorrect. Based on the current data, *M. terrestre* can be separated from *G. sinicum* nov. spec. by the following features: (i) the number of adoral membranelles (45–50 vs. 28–33); (ii) a paroral that commences at the same level as the endoral (vs. the paroral commences more anteriorly than the endoral); (iii) the numbers of right (17 vs. 21–35) and left (12 vs. 18–27) marginal cirri; (iv) the number of frontoventral rows (invariably three vs. three or four); (v) the number of cirri formed by anlage n−1 (ca. six vs. ca. ten); and (vi) the number of frontoterminal cirri (ca. ten vs. ca. six) (Fig. 5E, F; Alekperov 2005; Berger 2011; Foissner 2016).

Gonostomum sp. 1 was described in Shin's dissertation without providing a species-group name. It can be separated from *G. sinicum* nov. spec. by (i) its buccal cirrus distinctly anteriorly to the undulating membranes (vs. adjacent to the right anterior of the paroral); (ii) three oblique pseudo-pairs of frontoventral cirri (vs. absent); (iii) pretransverse ventral cirri (vs. absent); (iv) the number of transverse cirri (five vs. two); (v) the total number of frontoventral cirri (seven vs. 10–18); and (vi) frontoventral cirri confined to the frontal area vs. extending onto the postoral area (Fig. 5G; Berger 2011; Shin 1994).

Urosoma macrostomum was described by Gellért (1957) and still remains a species incertae sedis in *Gonostomum*. *Urosoma macrostomum* can be separated from *G. sinicum* nov. spec. by the following features: (i) a rather long paroral composed of densely spaced basal bodies (vs. short and composed of widely spaced basal bodies); (ii) an adoral zone composed of 19 vs. 28–33 membranelles; (iii) the number of frontoterminal cirri (three vs. 5–7); (iv) the total number of frontoventral cirri (one vs. 10–18); (v) a body length of 70 μm (vs. 100–125 μm in vivo); (vi) 18 (vs. 21–35) right and 13 (vs. 18–27) left marginal cirri; and (vii) the number of transverse cirri (four vs. two) (Fig. 5H; Berger 2011; Gellért 1957).

Gonostomum sinicum nov. spec. can be distinguished from *G. halophilum* by (i) the length of the paroral (8–15 μm vs. 0.5–2.0 μm); (ii) the length of the endoral (17–25 μm vs. 11–13 μm); (iii) the number of cirri formed by anlage n−1 (ca. ten vs. ca. five); and (iv) the total number of frontoventral cirri (10–18 vs. 7–9) (Fig. 6A; Foissner 2016).

Gonostomum sinicum nov. spec. differs from *G. salinarum* in (i) the total number of frontoventral cirri (10–18 vs. 6–9); (ii) the numbers of right (21–35 vs. 19–25) and left (18–27 vs. 13–17) marginal cirri; and (iii) the number of kinetids in dorsal kinety 2 (18–23 vs. 10–16) (Fig. 6B; Foissner 2016).

Gonostomum sinicum nov. spec. can be separated from *G. lajacola* by (i) the number of paroral kinetids (10–18 vs. 21–24); (ii) the arrangement of the frontoventral cirri in pseudo-pairs (absent vs. present); (iii) the number of frontoterminal cirri (5–7 vs. two); (iv) the total number of frontoventral cirri (10–18 vs. five or six); (v) the numbers of transverse and pretransverse ventral cirri (two vs. 5–7); (vi) the numbers of right (21–35 vs. 14–25) and left (18–27 vs. 10–15) marginal cirri; (vii) the length of the adoral zone (occupying 40–52% vs. 54–63% of body length); (viii) the length of the dorsal bristles (3–4 μm vs. up to 10 μm); and (ix) the size of the cortical granules (0.5 μm across vs. 3 × 1 μm) (Fig. 7C; Foissner 2016).

Gonostomum sinicum nov. spec. differs from *G. bromelicola* in (i) a continuous dorsal kinety 2 (vs. with distinct break); (ii) the arrangement of the frontoventral cirri in pseudo-pairs (absent vs. present); (iii) the number of frontoterminal cirri (5–7 vs. invariably two); (iv) the total number of frontoventral cirri (10–18 vs. five); (v) the numbers of right (21–35 vs. 15–22) and left (18–27 vs. 9–13) marginal cirri; (vi) the numbers of transverse and pretransverse cirri (two vs. seven); (vii) the number of adoral membranelles (28–33 vs. 34–43); (viii) the size of the cortical granules (0.5 μm across vs. 3–4 × 1 μm); (ix) the length of the adoral zone (occupying 40–52% vs. 48–64% of body length); and (x) the habitat (terrestrial vs. in tanks of bromeliads) (Fig. 6D; Foissner 2016).

Gonostomum sinicum nov. spec. differs from *G. fraterculus* in (i) the arrangement of the frontoventral cirri in pseudo-pairs (absent vs. present); (ii) the number of frontoterminal cirri (5–7 vs. invariably two); (iii) the total number of frontoventral cirri (10–18 vs. five); (iv) the numbers of transverse and pretransverse cirri (two vs. seven); (vi) the number of adoral membranelles (28–33 vs. 31–43); (vii) the size of the cortical granules (0.5 μm across vs. 3–4 × 1 μm); (viii) the length of the adoral zone (occupying 40–52% vs. 53–62% of body length); and (ix) the number of paroral kinetids (10–18 vs. 17–28) (Fig. 6E; Foissner 2016).

Variable number of frontoventral transverse cirral anlagen

The most striking morphogenetic feature of *G. sinicum* nov. spec. is its variable number of anlagen causing a variable number of frontoventral rows, i.e. the number of anlagen is five or six in different individuals (Fig. 2L–Q, 3G, 4A, E, G). In some dividers (two in nine), the number even differs between proter and opisthe in a way that the proter and opisthe possess six and five anlagen, respectively (Fig. 3E, 4C).

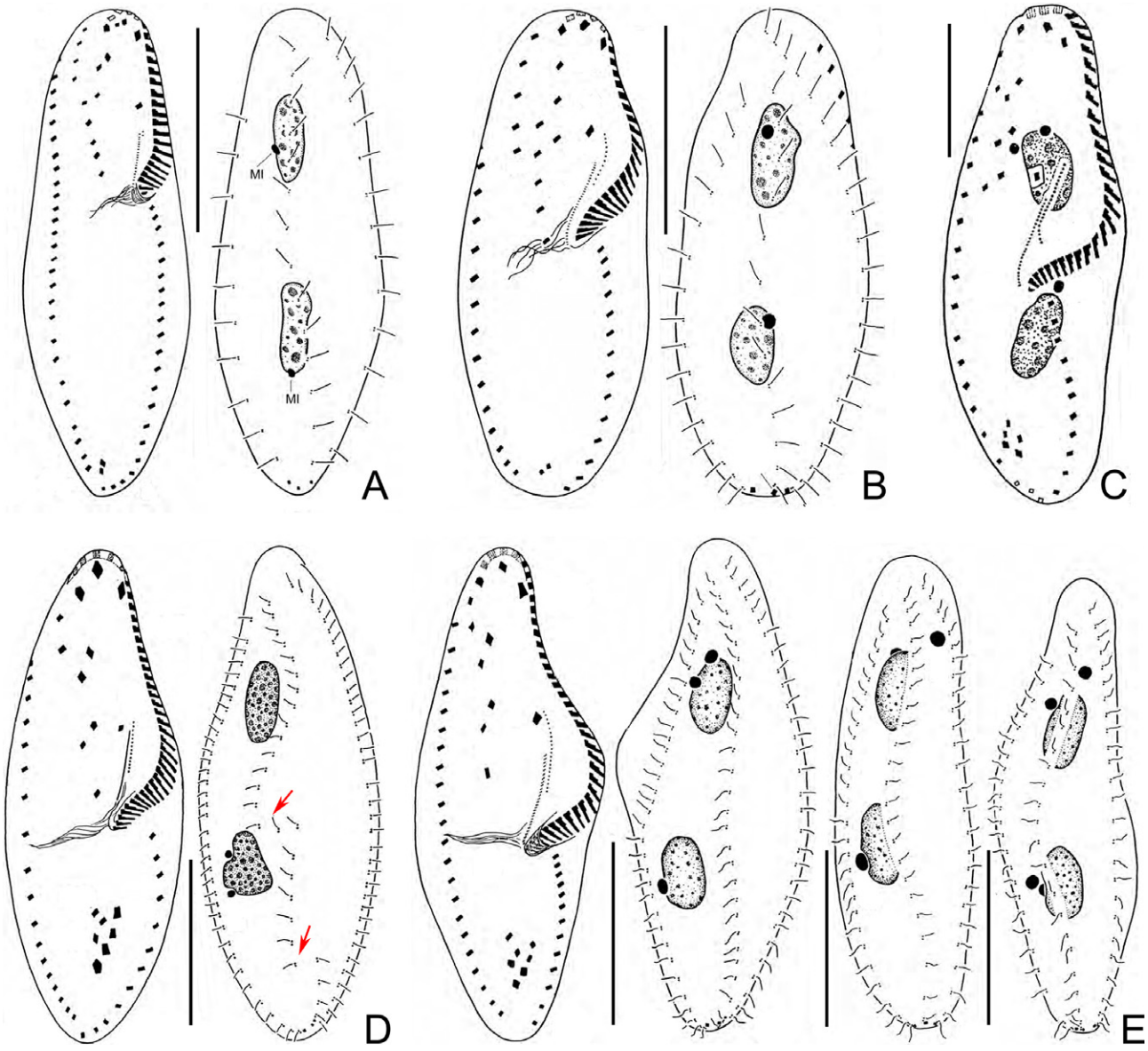

Figure 6 Infraciliature of species closely related with *Gonostomum sinicum* nov. spec. (**A**) *Gonostomum halophilum* (from Foissner 2016). (**B**) *Gonostomum salinarum* (from Foissner 2016). (**C**) *Gonostomum lajacola* (from Foissner 2016); (**D**) *Gonostomum bromelicola* (from Foissner 2016), arrows depict the distinct breaks in dorsal kinety 2; (**E**) *Gonostomum fraterculus* (from Foissner 2016). Scale bars = 30 μm (A, B, D, E); 20 μm (C).

In *Gonostomum*, an anlage usually originates from a parental structure which itself originated from the same anlage (Berger 2011). Based on this feature, there are three possibilities to explain the variation in number of anlagen: (i) when both daughter cells possess five anlagen, the parental cell probably is a three-frontoventral-rowed individual originally; (ii) when both daughter cells possess six anlagen, the parental cell is most likely to be a four-frontoventral-rowed individual originally; (iii) when the proter possesses six anlagen, while the opisthe of the same divider has only five, the parental cell probably is a four-frontoventral-rowed individual originally, in which anlage IV is not long enough to extend to the postoral area so that it cannot be distributed to the opisthe.

Morphogenetic comparison

Morphogenesis has been studied in eight *Gonostomum* species, i.e. *G. affine*, *G. algicola*, *G. kuehnelti*, *G. strenuum*, *G. salinarum*, *G. singhii*, *G. gonostomoidum*, and *G. bromelicola*. A uniform pattern emerged, viz., primary primordia are produced in early stages and later divide to form the individual anlagen for both filial products (Berger 2011; Foissner 2016). *Gonostomum sinicum* nov.

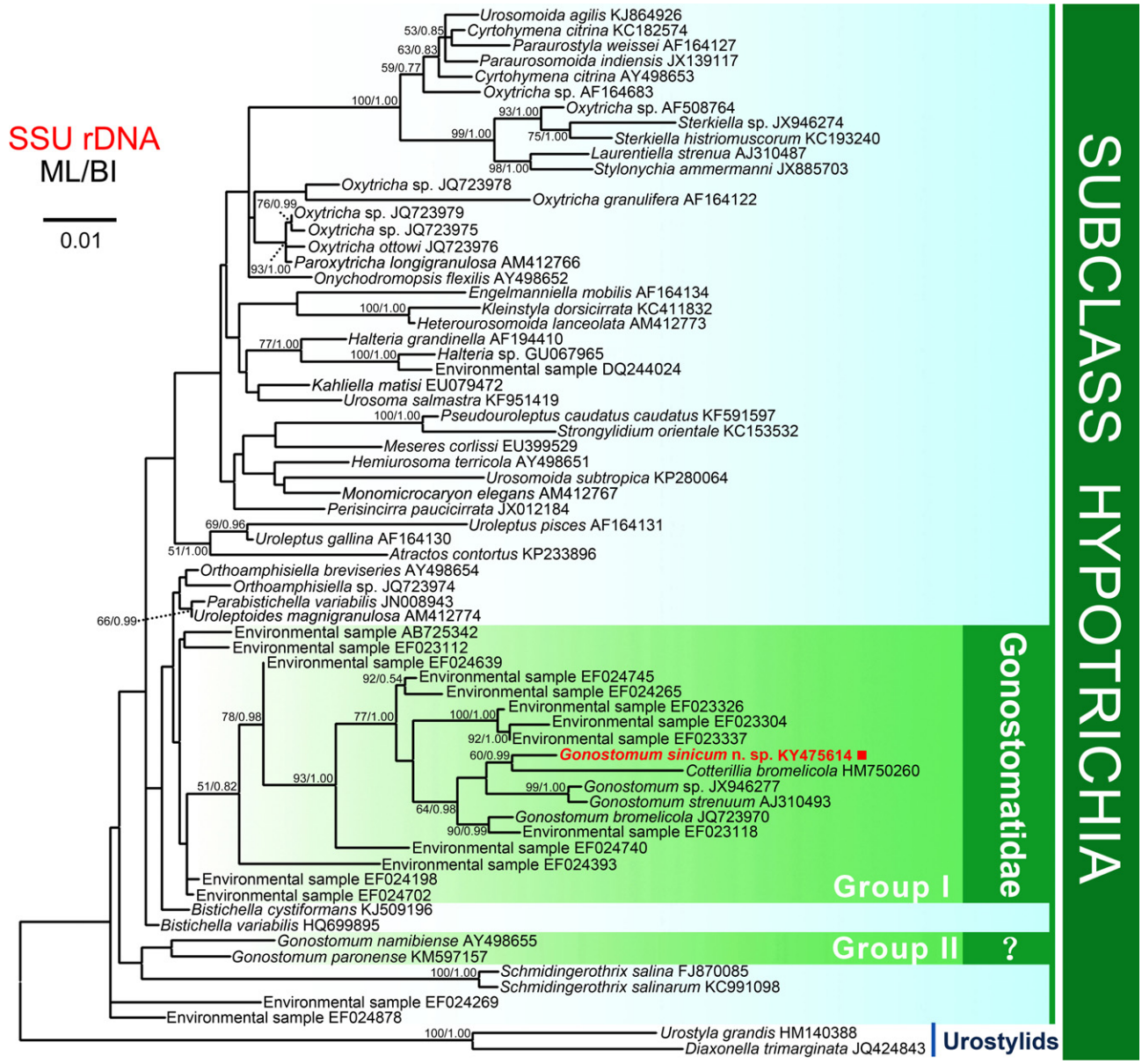

Figure 7 Maximum likelihood (ML) tree inferred from the SSU rDNA sequences showing the systematic position of *Gonostomum sinicum* nov. spec. (in bold). Bootstrap values above 50 for the Maximum likelihood (ML, 1,000 replicates) and/or Bayesian inference (BI, 1,000 replicates) are given at the individual nodes. All branches are drawn to the scale bar, which corresponds to one substitution per 100 nucleotide positions.

spec. corresponds well with this pattern, except for anlage I, which develops separately. However, according to Eigner (1999), the anlage I in *G. kuehnelti* is from a long primary primordium. This feature is not clearly recognizable from the published data and should thus be verified by further studies (Berger 2011).

It is also noteworthy to point out the unique dorsal development in *Gonostomum bromelicola*, i.e. its second dorsal kinety anlage undergoes fragmentation during the middle division stage and finally four dorsal kineties are formed (Foissner 2016). Surprisingly, this special pattern resembles the fragmentation of the third dorsal kinety anlage in oxytrichids (Berger 1999). However, other *Gonostomum* species unanimously follow the *Gonostomum* pattern, viz., do not show a fragmentation of the dorsal kinety anlage and only form three dorsal kineties (Berger 2011). Foissner and Stoeck (2008) confirm the validity of the CEUU (Convergent Evolution of Urostylids and Uroleptids) hypothesis, proving that dorsal fragmentation is a more important feature for inferring the phylogeny of hypotrichs. Thus, *G. bromelicola* obviously presents an exceptional state in *Gonostomum*.

Phylogenetic analyses

The new sequence obtained in this study and sequences from unidentified environmental samples provide the opportunity to further improve the phylogenetic analyses concerning the Gonostomatidae. As previously shown (Bharti et al. 2015; Foissner and Stoeck 2011), neither the family Gonostomatidae nor the genus *Gonostomum* are monophyletic. However, a well-recognized clade containing *G. sinicum* nov. spec., *Cotterillia*, *G. strenuum*, *G. bromelicola*, one unidentified *Gonostomum* species, and one unknown taxon from environmental samples emerged in all phylogenetic analyses we performed. The large number of unidentified environmental sequences further highlights the assumption that there is still a considerable proportion of ciliates to be discovered and described (Foissner and Stoeck 2008).

Gonostomum namibiense groups with *G. paronense*, forming a branch distinctly separated from the major cluster of gonostomatid species. Foissner (2016) established a new genus *Apogonostomum*, which refers to tailed Gonostomatidae with transverse cirri and frontoventral cirral pairs extending in body's midline to the buccal vertex or to the transverse cirri. Therefore, it is very likely that *G. namibiense* and *G. paronense* belong to the genus *Apogonostomum* as they can be easily distinguished from other species of *Gonostomum* by their tailed bodies and frontoventral cirral pairs (Bharti et al. 2015).

Gonostomum sinicum nov. spec. clusters with *Cotterillia bromelicola*; however, this relationship should not be over interpreted as the support values are variable in the ML and BI trees (ML/BI, 60/0.99). In addition, the molecular data of Gonostomatidae are only available from five identified *Gonostomum* species and *Cotterillia bromelicola* (Berger 2011; Bharti et al. 2015; Foissner 2016; Foissner and Stoeck 2011). Thus, the current taxon sampling is insufficient for unraveling a robust phylogeny of this complex group. Phylogenetic analyses based on multi-gene data as well as sequences of the type species (*G. affine*) are needed to provide further insights in the phylogeny of gonostomatid ciliates.

TAXONOMIC SUMMARY

Subclass Hypotrichia Stein, 1859
Family Gonostomatidae Small and Lynn, 1985
Genus *Gonostomum* Sterki, 1878

Gonostomum sinicum nov. spec.

Diagnosis. Size in vivo 100–125 × 30–40 μm. Outline in ventral view elliptical. Two macronuclear nodules, one or two micronuclei. Cortical granules colorless, ca. 0.5 μm across, arranged in short rows. Cytoplasm colorless to grayish. Contractile vacuole posterior to buccal vertex near cell midline. Adoral zone composed of 28–33 membranelles. Three enlarged frontal cirri. One buccal cirrus. Three or four frontoventral rows, row of frontoventral cirri extending onto postoral area. Usually two transverse cirri. One left and one right marginal row composed of 18–27 and 21–35 cirri, respectively. Three bipolar dorsal kineties in *Gonostomum* pattern. Three caudal cirri.

Type locality. Longfeng Wetland (46°35′30″N, 125°13′-08″E), Daqing, northern China (Supporting Information).

Type slides. The protargol-stained slide with the holotype specimen circled (Fig. 1D, E, 2G) by ink is deposited in the Laboratory of Protozoology, Ocean University of China (OUC, registration number: Leo201501050401). One paratype slide is deposited in the Natural History Museum, London, U.K. (registration number: NHMUK 2015.5.6.1).

Etymology. The species-group name *sinicum* refers to the country where the species was discovered.

ZooBank registration. Registration number of work: lsid: zoobank.org: pub: D62D5089-5F3F-4B29-B557-75F70EC42649.

ACKNOWLEDGMENTS

This work was supported by the Natural Science Foundation of China (Projects numbers: 31372148, 31401963, 31430077), the Fundamental Research Funds for the Central Universities (201564022) and Shaanxi Scientific Technological Coordination and Innovation Project (No. 2015KTTSNY01-07) and the Deanship of Scientific Research at King Saud University, prolific research group (PRG-1436-24). Many thanks are also due to Ms. Zhao Lv for her kind help with gene sequencing and to two anonymous reviewers and the AE.

LITERATURE CITED

Alekperov, I. K. 2005. Atlas of free-living infusoria (Class Kinetofragminophora, Colpodea, Oligohymenophora, Polyhymenophora). *Borcali, Baku, Azerbaijan*.

Berger, H. 1999. Monograph of the Oxytrichidae (Ciliophora, Hypotrichia). *Monogr. Biol.*, 78:i–xiii, 1–1080.

Berger, H. 2011. Monograph of the Gonostomatidae and Kahliellidae (Ciliophora, Hypotricha). *Monogr. Biol.*, 90:1–741.

Berger, H. & Foissner, W. 1988. The morphogenesis of *Kahliella franzi* (Foissner, 1982) nov. comb, and *Oxytricha gigantea* Horváth, 1933 (Ciliophora, Hypotrichida). *Arch. Protistenk.*, 136:65–77.

Bharti, D., Kumar, S. & La Terza, A. 2015. Two gonostomatid ciliates from the soil of Lombardia, Italy; including note on the soil mapping project. *J. Eukaryot. Microbiol.*, 62: 762–772.

Bourland, W. A. 2015. Morphology, ontogenesis and molecular characterization of *Atractos contortus* Vorosvary, 1950 and *Stichotricha aculeata* Wrzesniowskiego, 1866 (Ciliophora, Stichotrichida) with consideration of their systematic positions. *Eur. J. Protistol.*, 51:351–373.

Castresana, J. 2000. Selection of conserved blocks from multiple alignments for their use in phylogenetic analysis. *Mol. Biol. Evol.*, 17:5402–5552.

Chen, L., Lv, Z., Shao, C., Al-Farraj, S. A., Song, W. & Berger, H. 2015a. Morphology, cell division, and phylogeny of *Uroleptus longicaudatus* (Ciliophora, Hypotricha), a species of the *Uroleptus limnetis* complex. *J. Eukaryot. Microbiol.*, 63:349–362.

Chen, L., Zhao, X., Ma, H., Warren, A., Shao, C. & Huang, J. 2015b. Morphology, morphogenesis and molecular phylogeny of a soil ciliate, *Pseudouroleptus caudatus caudatus* Hemberger, 1985 (Ciliophora, Hypotricha), from Lhalu Wetland, Tibet. *Eur. J. Protistol.*, 51:1–14.

Dong, J., Lu, X., Shao, C., Huang, J. & Al-Rasheid, K. A. 2016. Morphology, morphogenesis and molecular phylogeny of a novel saline soil ciliate, *Lamtostyla salina* n. sp. (Ciliophora, Hypotricha). *Eur. J. Protistol.*, 56:219–231.

Eigner, P. 1999. Comparison of divisional morphogenesis in four morphologically different clones of the genus *Gonostomum* and update of the natural hypotrich system (Ciliophora, Hypotrichida). *Eur. J. Protistol.*, 35:34–48.

Fan, Y., Lu, X., Huang, J., Hu, X. & Warren, A. 2016. Redescription of two little-known urostyloid ciliates, *Anteholosticha randani* (Grolière, 1975) and *A. antecirrata* (Ciliophora, Urostylida). *Eur. J. Protistol.*, 53:96–108.

Fan, Y., Zhao, X., Hu, X., Miao, M., Warren, A. & Song, W. 2015. Taxonomy and molecular phylogeny of two novel ciliates, with establishment of a new genus, *Pseudogastrostyla* n. g. (Ciliophora, Hypotrichia, Oxytrichidae). *Eur. J. Protistol.*, 51:374–385.

Foissner, W. 2000. Notes on ciliates (Protozoa, ciliophora) from *Espeletia* trees and *Espeletia* soils of the Andean Páramo, with descriptions of *Sikorops espeletiae* nov. spec. and *Fragmocirrus espeletiae* nov. gen., nov. spec. *Stud. Neotrop. Fauna Environ.*, 35:52–79.

Foissner, W. 2014. An update of 'basic light and scanning electronmicroscopic methods for taxonomic studies ofciliated protozoa'. *Int. J. Syst. Evol. Microbiol.*, 64:271–292.

Foissner, W. 2016. Terrestrial and semiterrestrial ciliates (Protozoa, Ciliophora) from Venezuela and Galápagos. *Denisia*, 35:1–912.

Foissner, W., Agatha, S. & Berger, H. 2002. Soil ciliates (Protozoa, Ciliophora) from Namibia (Southwest Africa), with emphasis on two contrasting environments, the Etosha region and the Namib desert. Part I: Text and line drawings. Part II: Photographs. *Denisia*, 5:1–1459.

Foissner, W. & Stoeck, T. 2008. Morphology, ontogenesis and molecular phylogeny of *Neokeronopsis* (*Afrokeronopsis*) *aurea* nov. subgen., nov. spec. (Ciliophora: Hypotricha), a new african flagship ciliate confirms the CEUU hypothesis. *Acta Protozool.*, 47:1–33.

Foissner, W. & Stoeck, T. 2011. *Cotterillia bromelicola* nov. gen., nov. spec., a gonostomatid ciliate (Ciliophora, Hypotricha) from tank bromeliads (Bromeliaceae) with de novo originating dorsal kineties. *Eur. J. Protistol.*, 47:29–50.

Foissner, W., Stoeck, T., Schmidt, H. & Berger, H. 2001. Biogeographical differences in a common soil ciliate, *Gonostomum affine* (Stein), as revealed by morphological and RAPD-fingerprint analysis. *Acta Protozool.*, 40:83–98.

Gao, F., Warren, A., Zhang, Q., Gong, J., Miao, M., Sun, P., Xu, D., Huang, J., Yi, Z. & Song, W. 2016. The all-data-based evolutionary hypothesis of ciliated protists with a revised classification of the phylum Ciliophora (Eukaryota, Alveolata). *Sci. Rep.* doi:10.1038/srep24874.

Gellért, J. 1957. Néhány hazai lomblevelü és tülevelü erdö talajának ciliáta-faunája (Ciliatenfauna im Humus einiger ungarischen Laub- und Nadelholzwälder). *Ann. Inst. Boil. Tihany*, 24:11–34.

Gouy, M., Guindon, S. & Gascuel, O. 2010. SeaView version 4: a multiplatform graphical user interface for sequence alignment and phylogenetic tree building. *Mol. Biol. Evol.*, 27:221–224.

Hall, T. A. 1999. BioEdit: a user-friendly biological sequence alignment editor and analysis program for Windows 95/98/NT. *Nucleic Acids Res. Ser.*, 41:95–98.

Hemberger, H. 1985. Neue Gattungen und Arten hypotricher Ciliaten. *Arch. Protistenk.*, 130:397–417.

Hu, X. & Kusuoka, Y. 2015. Two oxytrichids from the ancient Lake Biwa, Japan, with notes on morphogenesis of *Notohymena australis* (Ciliophora, Sporadotrichida). *Acta Protozool.*, 54:107–122.

Huang, J., Chen, Z., Song, W. & Berger, H. 2014. Three-gene based phylogeny of the Urostyloidea (Protista, Ciliophora, Hypotricha), with notes on classification of some core taxa. *Mol. Phylogenet. Evol.*, 70:337–347.

Huang, J., Luo, X., Bourland, W. A., Gao, F. & Gao, S. 2016. Multigene-based phylogeny of the ciliate families Amphisiellidae and Trachelostylidae (Protozoa: Ciliophora: Hypotrichia). *Mol. Phylogenet. Evol.*, 101:101–110.

Kumar, S. & Foissner, W. 2015. Biogeographic specializations of two large hypotrich ciliates: *Australocirrus shii* and *A. australis* and proposed synonymy o*f Australocirrus* and *Cyrtohymenides*. *Eur. J. Protistol.*, 51:210–228.

Li, L., Zhao, X., Ji, D., Hu, X., Al-Rasheid, K. A., Al-Farraj, S. A. & Song, W. 2016. Description of two marine amphisiellid ciliates, *Amphisiella milnei* (Kahl, 1932) Horváth, 1950 and *A. sinica* sp. nov. (Ciliophora: Hypotrichia), with notes on their ontogenesis and SSU rDNA-based phylogeny. *Eur. J. Protistol.*, 54:59–73.

Lu, X., Shao, C., Yu, Y., Warren, A. & Huang, J. 2015. Reconsideration of the 'well-known' hypotrichous ciliate *Pleurotricha curdsi* (Shi et al., 2002) Gupta et al., 2003 (Ciliophora, Sporadotrichida), with notes on its morphology, morphogenesis and molecular phylogeny. *Int. J. Syst. Evol. Microbiol.*, 65:3216–3225.

Luo, X., Gao, F., Al-Rasheid, K. A., Warren, A., Hu, X. & Song, W. 2015. Redefinition of the hypotrichous ciliate *Uncinata*, with descriptions of the morphology and phylogeny of three urostylids (Protista, Ciliophora). *Syst. Biodivers.*, 13:455–471.

Lv, Z., Shao, C., Yi, Z. & Warren, A. 2015. A molecular phylogenetic investigation of *Bakuella*, *Anteholosticha*, and *Caudiholosticha* (Protista, Ciliophora, Hypotrichia) based on three-gene sequences. *J. Eukaryot. Microbiol.*, 62:391–399.

Lynn, D. H. 2008. The ciliated protozoa: Characterization, classification and guide to the literature, 3rd ed. Springer Press, Dordrecht.

Medlin, L., Elwood, H. J., Stickel, S. & Sogin, M. L. 1988. The characterization of enzymatically amplified eukaryotic 16S-like rRNA-coding regions. *Gene*, 71:491–499.

Nylander, J. 2004. MrModeltest v2. Program distributed by the author. *Evolutionary Biology Centre, Uppsala University,* 2.

Pan, X., Fan, Y., Gao, F., Qiu, Z., Al-Farraj, S. A., Warren, A. & Shao, C. 2016. Morphology and systematics of two freshwater urostylid ciliates, with description of a new species (Protista, Ciliophora, Hypotrichia). *Eur. J. Protistol.*, 52:73–84.

Penn, O., Privman, E., Ashkenazy, H., Landan, G., Graur, D. & Pupko, T. 2010. GUIDANCE: a web server for assessing alignment confidence scores. *Nucleic Acids Res.*, 38:W23–W28.

Ronquist, F. & Huelsenbeck, J. P. 2003. MrBayes 3: Bayesian phylogenetic inference under mixed models. *Bioinformatics*, 19:1572–1574.

Shin, M. K. 1994. Systematics of Korean hypotrichs (Ciliophora, Polyhymenophora, Hypotrichida) and molecular evolution of hypotrichs. Ph.D. Dissertation. Seoul National University, Seoul, Korea. Dissertation Seoul National University.

Singh, J. & Kamra, K. 2015. Morphology and molecular phylogeny of an Indian population of *Cyrtohymena citrina* (Ciliophora, Hypotricha), including remarks on ontogenesis of *Urosomoida-Notohymena-Cyrtohymena* group. *Eur. J. Protistol.*, 51:280–289.

Song, W. 1990. A comparative analysis of the morphology and morphogenesis of *Gonostomum strenua* (Engelmann, 1862) (Ciliophora, Hypotrichida) and related species. *J. Protozool.*, 37:249–257.
Stamatakis, A., Hoover, P. & Rougemont, J. 2008. A rapid bootstrap algorithm for the RAxML web servers. *Syst. Biol.*, 57:758–771.
Sterki, V. 1878. Beiträge zur Morphologie der Oxytrichinen. *Z. Wiss. Zool.*, 31:29–58.
Talavera, G. & Castresana, J. 2007. Improvement of phylogenies after removing divergent and ambiguously aligned blocks from protein sequence alignments. *Syst. Biol.*, 56:564–577.
Tamura, K., Stecher, G., Peterson, D., Filipski, A. & Kumar, S. 2013. MEGA6: molecular evolutionary genetics analysis version 6.0. *Mol. Biol. Evol.*, 30:2575–2579.
Vd'ačný, P. & Tirjaková, E. 2006. A new soil hypotrich ciliate (Protozoa, Ciliophora) from Slovakia: Gonostomum albicarpathicum nov. spec. *Eur. J. Protistol.*, 42:91–96.
Wilbert, N. 1975. Eine verbesserte technik der protargolimprägnation für ciliaten. *Mikrokosmos*, 64:171–179.
Zhang, Q., Yi, Z., Fan, X., Warren, A., Gong, J. & Song, W. 2014. Further insights into the phylogeny of two ciliate classes Nassophorea and Prostomatea (Protista, Ciliophora). *Mol. Phylogenet. Evol.*, 70:162–170.
Zhao, X., Gao, S., Fan, Y., Strüeder-Kypke, M. & Huang, J. 2015. Phylogenetic framework of the systematically confused *Anteholosticha-Holosticha* complex (Ciliophora, Hypotrichia) based on multigene analysis. *Mol. Phylogenet. Evol.*, 91:238–247.

SUPPORTING INFORMATION

Additional Supporting Information may be found online in the supporting information tab for this article:

Figure S1. Sampling sites.
Data S1. Sequences modifications methods.